Applied Clay Science 90 (2014) 88–95

Contents lists available at ScienceDirect

Applied Clay Science

journal homepage: www.elsevier.com/locate/clay

Research paper

# Adsorption of nisin on raw montmorillonite

Carolina Ibarguren [a,b,c], Pablo M. Naranjo [a], Christian Stötzel [b], M. Carina Audisio [a,d], Edgardo L. Sham [a,d], E. Mónica Farfán Torres [a,e,*], Frank A. Müller [b]

[a] Instituto de Investigaciones para la Industria Química–Consejo Nacional de Investigaciones Científicas y Técnicas (INIQUI–CONICET), Universidad Nacional de Salta, Avenida Bolivia 5150, A4408FVY Salta, Argentina
[b] Institute of Materials Science and Technology (IMT), Friedrich-Schiller-University of Jena, Loebdergraben 32, D-07743 Jena, Germany
[c] Facultad de Ciencias de la Salud, Universidad Nacional de Salta, Avenida Bolivia 5150, A4408FVY Salta, Argentina
[d] Facultad de Ingeniería, Universidad Nacional de Salta, Avenida Bolivia 5150, A4408FVY Salta, Argentina
[e] Facultad de Ciencias Exactas, Universidad Nacional de Salta, Avenida Bolivia 5150, A4408FVY Salta, Argentina

ARTICLE INFO

*Article history:*
Received 15 February 2013
Received in revised form 27 December 2013
Accepted 27 December 2013
Available online 24 January 2014

*Keywords:*
Nisin
Montmorillonite
Peptide/support interaction
Food biopreservative

ABSTRACT

The aim of the present work was to develop food-grade materials capable of releasing antimicrobial agents. Montmorillonite (Mt), a raw, abundant inexpensive clay mineral approved as a food additive, was used as support material. The immobilized antimicrobial agent was pure nisin (Danisco, UK). A series of antibacterial compounds were prepared, and the antimicrobial activity of the resultant montmorillonite–nisin (MtNis) immobilized systems was determined against *Enterococcus faecium* C1. The characterization of the antimicrobial powders showed evidences of nisin adsorption on by means of a "frustrated intercalation" model with a nisin loading (NL) saturation value close to 0.24 CEC (cation exchange capacity) of Mt. The antibacterial powders with NL above this value completely inhibited *E. faecium* C1 during 24 h of contact. These results are encouraging for the development of nisin-based bioprotectors immobilized on raw Mt.



## 1. Introduction

Protein immobilization on solid surfaces is of particular interest for biomedical, technological and environmental applications (Servagent-Noinville et al., 2000). The interactions that occur during the immobilization process might obviously affect various characteristics of the immobilized protein. Nonetheless, the substrate surface plays an essential role in thermodynamics and kinetics (Reslow et al., 1988). Therefore, the choice of the support is crucial for preserving adequate biocompatibility.

Montmorillonite (Mt) is one of the most studied clay minerals of the smectite group. Its basic structure consists in a layer containing a central alumina octahedral sheet between two tetrahedral silica sheets which admits isomorphous substitutions, causing a net negative charge on the clay mineral surface counter balanced by exchangeable cations in the interlayer space. Also, weak electrostatic forces link together the parallel layers, allowing water and other molecules to intercalate into the interlayer space of clay mineral (Bergaya et al., 2006). This makes clay minerals good candidates as harmful substance adsorbents. Raw clay minerals have been utilized to immobilize amino acids, proteins and enzymes, the main purpose being the preparation of biosensors and biocatalysts. Additionally, the ingestion of clay minerals (geophagy) by humans and animals has been well-documented for a variety of beneficial purposes, e.g. as gastrointestinal protectors, mineral nutrients/supplements, and reducers of excess acidity in the digestive tract (Carretero et al., 2006; Kikouama et al., 2009; Wang et al., 2005). On the other hand, the FDA (American Food and Drug Administration) as well as the EFSA (European Food Safety Authority), consider raw clay minerals as safe food additives. Therefore, these materials might be suitable for the preparation of potential antibacterial protectives for food.

Nisin is a polypeptide bacteriocin produced by *Lactococuslactis* subsp. *lactis*. It presents antimicrobial activity against microorganisms that can cause food spoilage, and against food-associated pathogens such as *Clostridium botulinum*, *Bacillus cereus* and *Listeria monocytogenes*. It is a food additive (E234) approved by the Food and Agriculture Organization/World Health Organization (FAO/WHO). It is also part of the FDA list of GRAS (generally recognized as safe) additives, which means that its use in food is safe and harmless for humans (Thomas and Delves-Broughton, 2005). Nisin is a cationic and hydrophobic polypeptide with a molar mass of 3500 Da. It consists of 34 amino acids including three lysine and two histidine residues (Chandrapati and O'Sullivan, 1998). The protonation of these residual amino groups could favor electrostatic interactions between nisin molecules and negatively-charged surfaces of the clay mineral.

In recent years, a growing demand for fresh, natural and minimally processed food has drawn public attention towards the use of alternative

* Corresponding author at: INIQUI–CONICET, Universidad Nacional de Salta, Avenida Bolivia 5150, A4408FVY Salta, Argentina. Tel./fax: +54 3874251006.
*E-mail addresses:* cibar@unsa.edu.ar (C. Ibarguren), pnaranjo@unsa.edu.ar (P.M. Naranjo), christian.stoetzel@uni-jena.de (C. Stötzel), audisio@unsa.edu.ar (M.C. Audisio), sham@unsa.edu.ar (E.L. Sham), mfarfan@unsa.edu.ar (E.M. Farfán Torres), frank.mueller@uni-jena.de (F.A. Müller).

0169-1317/$ – see front matter © 2014 Elsevier B.V. All rights reserved.
http://dx.doi.org/10.1016/j.clay.2013.12.031

natural biopreservatives such as lactic bacteria bacteriocins (Deegan et al., 2006). Biopreservation utilizes antagonistic microorganisms and their metabolic products to inhibit undesirable bacteria in food and, consequently, to improve its safety and/or to prolong its shelf-life (Chen and Hoover, 2003). The direct introduction of antimicrobials into food products is accompanied by an undesired dilution effect and a possible interaction between different food components. This might result in a decrease of the antagonistic action on the target cells. Therefore, the analysis of alternative methods that can overcome these difficulties may improve the antimicrobial activity and stability of biopreservatives in complex systems (Were et al., 2004).

The nisin immobilization process has been studied using different methods: mainly adsorption on solid supports and encapsulation in polymeric matrices (Bower et al., 1995; Daeschel et al., 1992; Lante et al., 1994). The supports used for the immobilization of this polypeptide are: silica of different origins for surface deposition (Bower et al., 1995; Dawson et al., 2005; Janes et al., 1998), and inorganic and organic polymers for the encapsulation process (Benech et al., 2002; Cutter and Siragusa, 1997; Lante et al., 1994). To the best of our knowledge, there are no reports regarding the use of clay mineral as support for the deposition of nisin. Previous studies have shown that immobilized nisin conserved a good antimicrobial activity when slightly hydrophobic supports such as synthetic silica were used (Bower et al., 1995; Dawson et al., 2005; Liu and Jansen, 1990). Raw clay minerals, such as Mt, have numerous advantages qualifying them for this application: they have low cost, they are already used as food additives and they have already been used successfully as vehicles for the controlled release of active ingredients of drugs (Joshi et al., 2009).

In this work, the adsorption of nisin on raw Mt and the interaction between the peptide and the support matrix was evaluated. The aim was to develop food-grade materials with immobilized nisin capable of releasing the antimicrobial agent.

## 2. Experimental section

### 2.1. Support

A commercial raw Mt obtained from a mine in province of Río Negro (Argentina) was used as inorganic support. The chemical composition (53.40 $SiO_2$%, 17.95 $Al_2O_3$%, 4.75 $Fe_2O_3$%, 3.35 $Na_2O$%, 1.08 CaO%, 2.80 MgO%, 0.26 $K_2O$%, 0.37 $TiO_2$%, 0.05 BaO%,0.04 MnO%,0.01 $Cr_2O_3$%,0.06 $P_2O_5$%), structural formula ($[(Si_{3.89}\ Al_{0.11}), (Al_{1.43}\ Fe_{0.26}\ Mg_{0.30})]\ M^{+}{}_{0.41}$) and mineralogical composition (84% Mt, 12% feldspar, 4% quartz) of this clay mineral was determined by Magnoli et al. (2008). The cation exchange capacity (CEC) of this Mt, measured by the copper bis-ethylenediamine complex method (Bergaya and Vayer, 1997), was established as 83.7 mmol/100 g by Naranjo (2012).

The monosodium Mt fraction (≤2 μm) of the clay mineral was obtained by saturation with NaCl, after rinsing several times with distilled water and centrifugation (12,000 rpm for 10 min). The purified $Na^+$–Mt thus prepared was dispersed in distilled water and the final concentration was established as 29.2 mg/mL by total suspended solids determination using an oven drying (110 °C).

### 2.2. Peptide solutions (adsorbate)

The immobilized antimicrobial agent was pure nisin (Danisco, UK). Nisin solutions (5 mg/mL) were prepared in sterilized water, filter-sterilized (0.45 μm) and kept at 8 °C until used for the immobilization assays.

The antimicrobial activity of nisin was determined by the serial 1:2 dilution method (Daba et al., 1991), using *Enterococcus faecium* C1 as the indicator strain. Briefly, molten brain heart infusion (BHI) agar was inoculated (1% v/v) with overnight grown cells (ca. $10^6$ cfu/mL), poured into Petri dishes and dried for 30 min. Nisin solutions were two-fold serially diluted in sterile distilled water and 20 μL aliquots of each dilution were applied in 5 mm wells made in the BHI agar plates. The plates were incubated at 25 °C for 20 h. The nisin titer was expressed in arbitrary units per milliliter (AU/mL) and calculated as follows: $(1000)/(V_s \times D)$, where $V_s$ is the tested bacteriocin volume and D represents the highest dilution that still inhibits cell growth. The titer determined for nisin (5 mg/mL) solution was 25,600 AU/mL.

### 2.3. Preparation of nisin immobilized systems

A series of antibacterial compounds were prepared by mixing different amounts of the Mt dispersion with a nisin (5 mg/mL) aqueous solution. After 2 h of stirring at 25 °C, the solids were recovered by centrifugation (10 min, 1000 *g*, 25 °C), rinsed with distilled water and freeze-dried prior to further characterization.

The concentration of nisin in each montmorillonite–nisin (MtNis) system was determined as the fraction of CEC satisfied by nisin molecules (Redding et al., 2002):

$$\mathbf{NL} = \mathbf{gNis}/(\mathbf{CEC} \cdot \mathbf{gMt} \cdot \mathbf{MNis} \cdot \mathbf{XNis})$$

where **gNis** is the nisin mass required to achieve the desired fraction of CEC, **gMt** is the Mt mass, **MNis** is the gram molecular mass of nisin, and **XNis** are the moles of charge per mol of nisin (taken as 1 at this point for sample labeling).

The antibacterial compounds were designed in order to achieve nisin loadings (NL) equivalent to a $CEC_{Mt}$ of 0.06, 0.12, 0.24, 0.60 and 1.21, respectively. The resulting MtNis systems were labeled according to these NL values.

### 2.4. Antimicrobial activity

The residual antimicrobial activity of supernatants that were obtained by centrifugation (10,000 *g*, 10 min) after contact with the solid was determined by the serial 1:2 dilution method using *E. faecium* C1 as indicator strain (described in section 2.2).

In addition, the inhibitory activity of Mt immobilized nisin was assayed using two methods: the agar diffusion technique and the direct contact method. Both assays were carried out thrice.

#### 2.4.1. Agar diffusion

A modified agar diffusion technique was used to determine the activity of encapsulated bacteriocins against *E. faecium* C1 (Audisio et al., 2005). For this purpose, the agar wells were loaded with lyophilized MtNis systems and the inhibition halo zones were measured after 24 h incubation at 37 °C.

#### 2.4.2. Direct contact in microplates

An adapted version of the direct contact technique was used (Ibarguren et al., 2010). One milliliter of a dispersion of *E. faecium* C1 (ca. $10^6$ cfu/mL) in peptone water was added to different series of lyophilized MtNis systems. The strain viability was determined after 0, 1, 2, 6 and 24 h of incubation (25 °C) through cell counts on BHI agar plates. A dispersion of the strain in contact with lyophilized Mt without nisin was used as growth control.

### 2.5. Characterization of the nisin-support systems

Mt and MtNis samples were characterized by X-ray diffraction (XRD) (Bruker AXS D8 Discover, USA) using Cu Kα radiation. Continuous scans were performed in the 2θ range between 3° and 70°, with a normal speed of 2°/min, and the diffractometer operating at 40 kV and 40 mA. In the cases where overlapping peaks were detected, mathematical deconvolutions were performed using the OriginPro© 8 software (OriginLab Corporation, USA). The positions and peak areas were calculated applying a Gaussian peak-fitting algorithm for nonlinear least-squares (Naranjo et al., 2013).

Small amounts of the freeze-dried powders were disposed on sticky carbon tapes and then sputter-coated with a thin Au layer (1 min, 20 mA) (Edwards 515OB Sputter Coater, UK). The samples were characterized by scanning electron microscopy (SEM) (Leica S440i, Japan) at 15 kV. Elemental analysis of single particles was performed using energy-dispersive X-ray (EDX) diffraction (EDX, Oxford 5431, UK).

Small drops of ethanol (50% v/v) dilute dispersions of the samples were placed on Cu mesh grids coated with a thin carbon film. The grids were air-dried prior to insertion into the transmission electronic microscope (JEOL JEM 3100, Japan). The samples were examined at an accelerating voltage of between 200 and 300 kV.

X-ray photoelectron spectroscopy (XPS) analyses were performed using a photoelectron spectrometer (Quantum 2000, Physical Electronics Instruments, USA) with an Al Kα X-ray source (h = 1486.6 eV) operating at $P = 1 \times 10^{-10}$ Torr. Spectra were carried out with 20 eV pass energy for the survey scan and 10 eV pass energy for the $C_{1s}$, $N_{1s}$, $O_{1s}$, $Na_{1s}$, $Al_{2p}$, $Si_{2p}$, $S_{2p}$, and $Cl_{2p}$ regions.

Fourier transform infrared (FTIR) spectra were recorded with a Pt single reflection diamond attenuated total reflectance (ATR) module (Bruker Alpha, USA). The scans were collected over the 375 to 4000 $cm^{-1}$ wavenumber range.

The surface charge of Mt, Nisin and the MtNis systems was determined from the electrophoretic mobilities measured at 25 °C using a Zetasizer (Malvern ZEN3600, UK) in connection with a multipurpose autotitrator (model MPT-2, Malvern UK). Appropriate amounts of the solids (ca. 0.01%mass/v) were dispersed in 0.01 M KCl to maintain a constant ionic strength, and were ultrasonically stirred several times in order to ensure the stabilization of the clay mineral before each measurement. Titration was performed from pH 2.0 to pH 11.0 using 0.01 M HCl and KOH under constant magnetic stirring. The reported data refer to average values of three measurements performed with three individually prepared dispersions.

For thermodifferential (DTA) and thermogravimetric (TG) analyses, 5 mg (TG) and 10–30 mg (DTA) of ground samples were heated in a platinum crucible from 10 to 1000 °C at 10 °C/min under a static air atmosphere (Shimadzu TGA 50H/DTA50 Thermal Analyzer, Japan).

## 3. Results and discussion

### 3.1. Antimicrobial activity

Antimicrobial activity was detected in the supernatants recovered by centrifugation after contact with the MtNis powders. The residual nisin activity decreased with the increase of Mt content of the immobilized system. The initial 25,600 AU/mL titer of the 5 mg/mL nisin solution decreased to 6400, 3200, 400, 100 and 50 AU/mL for the supernatants after contact with MtNis1.21, MtNis0.60, MtNis0.24, MtNis0.12, and MtNis0.06, respectively.

Although the MtNis systems with lower NL showed almost complete adsorption of nisin (low antimicrobial activity in supernatants), the inhibitory activity of the resulting MtNis powders illustrated major inhibitory effect of systems with higher NL in a solid medium (Fig. 1a). This means that for low NL the adsorbed peptide does not contribute to the antimicrobial activity, probably because it is more strongly adsorbed on the support. This was confirmed by results from direct-contact experiments (Fig. 1b). *E. faecium* C1 cell count decreased during the first 6 h of contact with MtNis0.06, 0.12 and 0.24 immobilized systems, compared with the growth of the control strain in absence of adsorbed nisin. This inhibition effect diminished with exposure time, and the viability of the cells in contact with these systems reached values similar to those of the growth control after 24 h. Even so, MtNis0.60 and 1.21 powders completely inhibited *E. faecium* C1; the viability dropped to values below the cell count detection limit ($<10^2$ ufc/ml) as soon as the immobilized systems were in contact with the cell dispersion. This effect was sustained for 24 h. These results show that nisin immobilized on Mt presents a NL critical value below

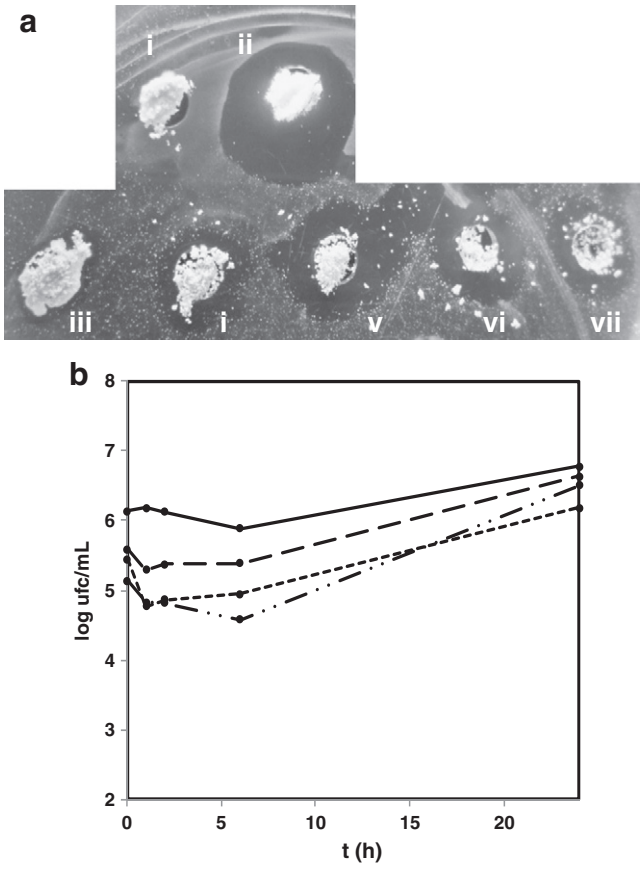


**Fig. 1.** (a) Inhibition halos of nisin (MtNis) freeze-dried immobilized systems against *E. faecium* C1, according to the agar diffusion technique. i) Mt (control), ii) nisin (control), iii) MtNis 0.06, iv) MtNis 0.12, v) MtNis 0.24, vi) MtNis 0.60, vii) MtNis 1.21. (b) *E. faecium* C1 viability in peptone water in contact with Mt (full line), MtNis 0.06 (— — —), MtNis 0.12 (——), MtNis 0.24 (— —••), freeze-dried immobilized systems, according to the direct contact bioassay.

which the peptide loses its antimicrobial activity. For the assayed conditions a NL > 0.24 was necessary to achieve the desired inhibitory effect versus *E. faecium* C1.

### 3.2. Characterization of the nisin support systems

XRD patterns were used to analyze the characteristic *d*(001) value of Mt. This value represents the thickness of the clay platelet plus the interlayer distance (Bertagnolli et al., 2011; Eloussaief et al., 2011; He et al., 2007; Zhou et al., 2008). In the case of organoclays, changes of this basal reflection generally indicate an intercalation of organic cation molecules within the interlayer space of the solid, with a high correlation for *d*(001) values of ion-exchanged raw clays with the same intercalants (Carrado, 2000; Yang et al., 2007). As shown in Fig. 2, a diffraction line at $2\theta = 9°$ corresponding to an interlayer space of 0.98 nm was observed in the clay mineral prior to the adsorption process. Once in contact with pure nisin, the systems showed the presence of two *d*(001) diffraction lines: one signal similar to the original Mt interlayer space, and a second line at lower angles indicating a modification of the Mt interlayer space distance after contact with the peptide solution due to an intercalation of the nisin molecules in the solid matrix.

SEM micrographs of the surface morphology of Mt and of the antimicrobial-Mt samples are shown in Fig. 3. Mt consists of rough flakes with a smooth surface (Fig. 3a), while the surface of the clay mineral treated with the antimicrobial peptide showed a more granular aspect (Fig. 3b and c).

TEM images of Mt, MtNis0.6 and MtNis0.60 systems are shown in Fig. 3d, e and f respectively. TEM is a technique used for clay minerals

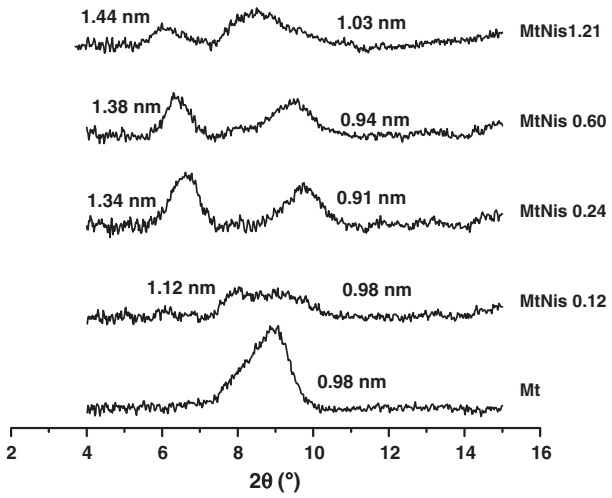


**Fig. 2.** XRD patterns of MtNis resulting systems.

that displays the packing density of adsorbed modified clays within the clay interlayer space (He et al., 2006b; Park et al., 2011). An increase in the $d(001)$ value for the MtNis antimicrobial solids was measured from TEM micrographs. Mt had an initial interlayer space of 0.95 nm. The $d(001)$ space increased to 1.22 nm and 1.36 nm for MtNis0.06 and MtNis0.60, respectively. This is in good agreement with the $d(001)$ space measured by XRD (0.98, 1.12, 1.44 nm for Mt, MtNis0.06 and MtNis0.60, respectively). Fig. 3g gives a general view of the MtNis0.60 powder. Irregular interlayer spaces are observed, in accordance with the double $d(001)$ signal detected by XRD.

Although the Mt interlayer space slightly increased with the increase of NL, this change (<0.50 nm), measured for the different MtNis systems, suggests that nisin molecules, or at least a part of them, are arranged parallel to the layer surface upon intercalation. This is similar to a "monolayer" accommodation, usually observed in the intercalation of alkyl ammonium surfactants on clays (Lagaly et al., 2006; Zhu et al., 2003). Considering the size of the nisin molecules (3 kDa), it seems unlikely that more than one molecule intercalates between the Mt layers, adopting bilayer, pseudo-trilayer or paraffin complex arrangements (Lagaly et al., 2006; Zhu et al., 2003). Even the introduction of whole nisin molecules in-between the silica layers is improbable. The modification of interlayer space suggests that the cationic portions of the nisin molecule interact with the clay mineral structure, producing a "frustrated intercalation" similar to the arrangement observed in organoclays prepared with certain dendritic surfactants (Acosta et al., 2003). This "frustrated intercalation" arrangement also explains the $d(001)$ values observed in MtNis XRD patterns, corresponding to both intercalated layers located near the edges of the clay mineral where nisin molecules have easy access, and to internal non-intercalated layers that cannot be reached by the antimicrobial agent.

Table 1 summarizes the results of the XPS analyzes concerning the elemental atomic concentrations of Mt, Nisin, MtNis0.12 and MtNis1.21. The results clearly indicate the presence of sodium, aluminum, silicon and oxygen in Mt, and of carbon, nitrogen, sulfur and oxygen in nisin. The increase in the nitrogen and carbon content, together with the increase in the O/Al and O/Si ratios with increasing NL, indicates an increment of the organic content in the resultant antimicrobial compounds. A decrease of the Al/Si ratio is expected when an intercalation of organic compounds occurs in clays. This intercalation increases interlayer space distance, leading to a decreasing possibility of detecting the Al–O(OH) octahedral layers sandwiched between the two Si–O tetrahedral layers of the Mt (He et al., 2007).

The XPS results are in good agreement with the elemental analyses of the same samples determined by EDX (Table 2). The increase in sulfur and chlorine contents when NL increases, indicates an increasing content of organic matter in the resulting MtNis system, since the peptide was the only source of these elements. In addition, the decrease of sodium content with increasing NL could result from the exchange of sodium ions by nisin cations (He et al., 2007). Moreover, the sodium signals disappeared at NL values between 0.12 CEC and 0.24 CEC, probably at an NL of 0.20. This means that one molecule of nisin displaces five molecules of Mt intercalated sodium, and that a NL equivalent to 20% of the clay CEC (i.e. 0.20 CEC) is needed for the complete displacement of sodium. Therefore, nisin molecules carry over the exchange reaction through its five cationic residues.

In the case of "frustrated intercalation", intercalated sodium should compensate the exchange sites in the central area of the clay mineral sheet. But the complete displacement detected by XPS and XRD measurements indicates that the presence of intercalated nisin, occupying regions close to the edges, could repel and eject sodium ions from those central sites of exchange. Beyond that, the intercalated antimicrobial peptide creates a more hydrophobic environment. As a consequence, sodium ions are more attracted to the solution than to the clay mineral sheets. This could be the explanation for some collapsed sheet areas observed in TEM micrographs (Fig. 3f, circle).

The FTIR spectra of the raw clay mineral, of nisin and of the different MtNis powders are shown in Fig. 4. The clay mineral spectra show a band at 995 $cm^{-1}$, assigned to Si – O and Si – O – Si stretching vibrations, as well as shoulders at 890 $cm^{-1}$ which represent Al – OH bending vibrations (He et al., 2006a). The band at 3622 $cm^{-1}$ is associated with the inner Si–OH signal; the broad undefined band between 3000 and 3500 $cm^{-1}$ corresponds to adsorbed water while bound interlayer water appears at 1635 $cm^{-1}$ (Acosta et al., 2003; Zhou et al., 2007). In the case of the peptide, the more pronounced signals correspond to the amide I (1638 $cm^{-1}$, stretching vibrations of the C═O bond) and amide II (1520 $cm^{-1}$ bending vibrations of the N – H bond) bands (Kong and Yu, 2007). The clay mineral signals were also observed in the MtNis antimicrobial systems. A slight shift of the band at 995 $cm^{-1}$ to higher wavelengths reflects interactions between the peptide and the Mt Si–O tetrahedral layers upon intercalation. No effect on the more internal Al–O octahedral layer was detected, as the signal near 890 $cm^{-1}$ was not altered (He et al., 2006a). Both nisin amide signals were also detected in the MtNis spectra. Normally, the analysis of the effect on bonded water provides a way to check if the intercalation occurs. Interlayer bonded water molecules are supposed to be displaced by the organic molecule upon intercalation, while organoclays displaying frustrated intercalation preserve the interlayer water (Acosta et al., 2003). In this case, the effect on bonded water in MtNis powders could not be seen clearly since the pure nisin amide I band (1638 $cm^{-1}$) and the adsorbed water band (~3300 $cm^{-1}$) superimposed with the interlayer bonded water signals.

The Zeta potential (ZP) titration curves of Mt, nisin and MtNis systems are shown in Fig. 5. The surface charge of Mt remained negative between pH 2 and 11. This can be explained by the highly negatively charged surface of silicates. As the NL increased in the MtNis systems, the surface charge became less negative and even reached positive values at low pH values. Finally, the MtNis1.21 antimicrobial compound behaved similar to the pure nisin dispersion. Again, a difference was observed for MtNis when NL exceeded 0.20. Positive ZP values were only measured for MtNis0.24, 0.60 and 1.21 for pH < 4. These detected differences on ZP profiles between the Mt and the MtNis systems confirmed that the adsorption of nisin molecules on the clay mineral did occur and that it modified its surface charge.

Fig. 6 shows the thermographic profiles of Mt, nisin and the different MtNis systems. The thermograms clearly indicate an increase in the amount of calcined organic matter (OM) when NL values increase. The TG–DTA profile obtained for Mt was similar to those previously reported for this type of clay mineral (Eloussaief et al., 2011; Naranjo et al., 2013). The endothermic peak at 93 °C can be assigned to the loss of water. Between 93 °C and 570 °C a further loss of adsorbed water without any thermal changes was observed, while the loss of structural

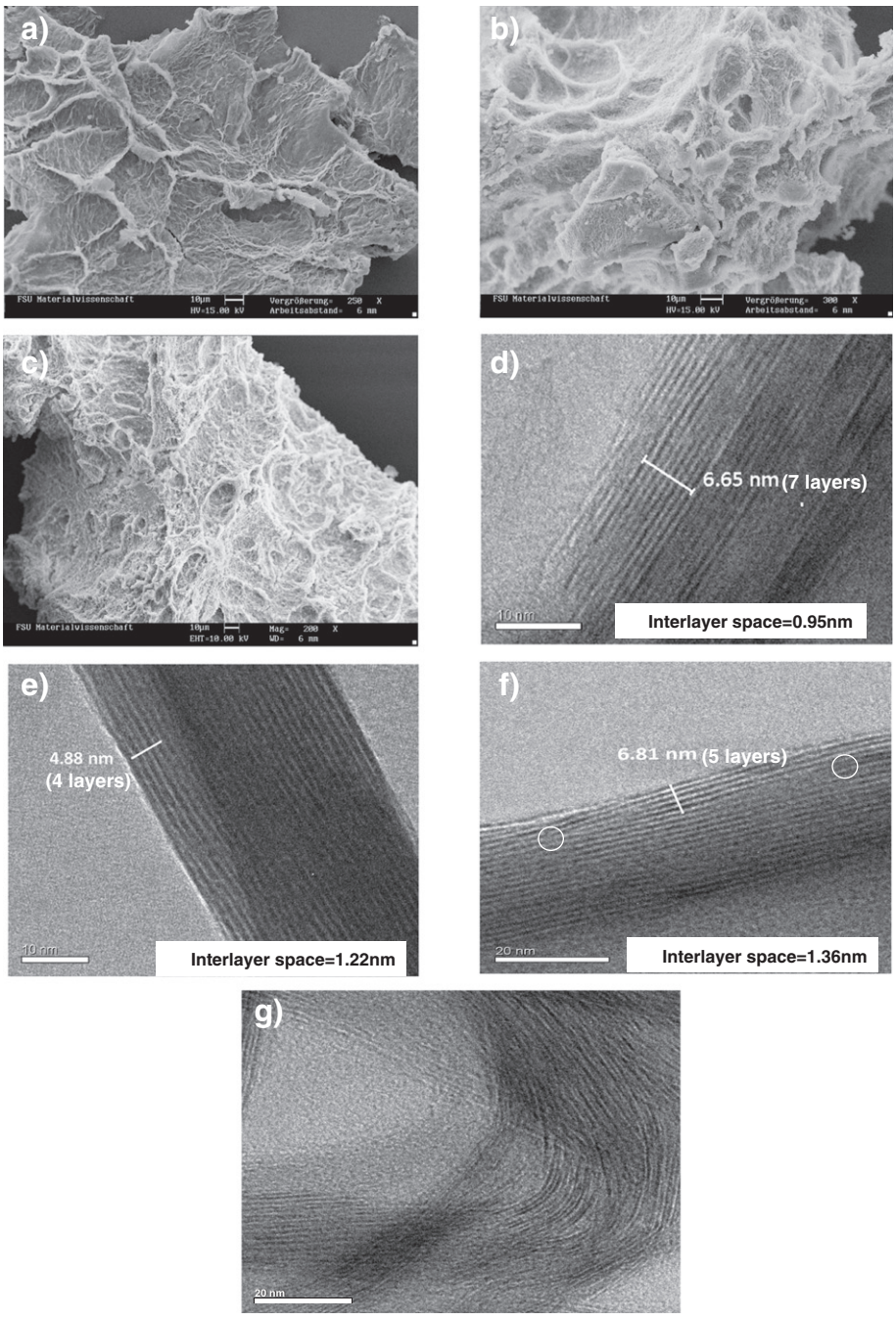


**Fig. 3.** SEM micrographs of a) Mt (250×, bars 10 μm), b) MtNis 0.06 (300×, bars 10 μm) and c) MtNis 0.60 (400×, bars 10 μm) systems. TEM micrographs of d) Mt (bars 10 nm), e) MtNis 0.06 (bars 10 nm), f) and g) MtNis 0.60 (bars 20 nm).

hydroxyl groups started at 570 °C. Finally, the exothermic peak at 900 °C can be associated with the rearrangement of high-temperature silica phases (Čičel and Kranz, 1981; Dellisanti et al., 2006). For pure nisin, the TG profile is characterized by a water loss at 80 °C (endothermic peak, adsorbed water) and between 80 and 240 °C (no associated

**Table 1**
Atomic percent weight of Mt and nisin, and atomic percent weight and ratios of the resultant MtNis antimicrobial clays based on XPS analyses.

| | Atomic mass (%) | | | | | | | Atomic mass (%) ratios | | |
|---|---|---|---|---|---|---|---|---|---|---|
| Sample | $C_{1s}$ | $N_{1s}$ | $S_{2p}$ | $Si_{2p}$ | $Al_{2p}$ | $O_{1s}$ | $Na_{1s}$ | O/Al | O/Si | Al/Si |
| Mt | 14.4 | 0.0 | 0.0 | 19.3 | 8.2 | 56.9 | 1.1 | – | – | – |
| Nisin | 64.7 | 16.4 | 1.9 | 0.4 | 0.0 | 16.1 | 0.0 | – | – | – |
| MtNis 0.12 | 21.8 | 5.1 | 0.0 | 13.7 | 3.3 | 54.8 | 1.2 | 16.9 | 4.0 | 0.24 |
| MtNis 1.21 | 36.4 | 10.5 | 0.6 | 9.3 | 1.9 | 41.3 | 0.0 | 20.9 | 4.5 | 0.20 |

**Table 2**
Elemental weight of Mt, nisin and the resultant MtNis antimicrobial clays based on EDX analyses.

| | Atomic mass (%) | | | | | |
|---|---|---|---|---|---|---|
| Sample | Na | Al | Si | S | Cl | Mg |
| Mt | 6.0 | 20.4 | 59.3 | 0.0 | 0.0 | 3.3 |
| Nisin | 0.0 | 0.0 | 2.0 | 35.7 | 61.4 | 0.0 |
| MtNis 0.06 | 4.4 | 20.4 | 61.1 | 0.0 | 0.0 | 3.2 |
| MtNis 0.12 | 3.0 | 20.4 | 61.9 | 0.4 | 0.0 | 3.1 |
| MtNis 0.24 | 0.0 | 20.7 | 64.7 | 1.4 | 0.0 | 2.9 |
| MtNis 0.60 | 0.0 | 20.3 | 62.8 | 2.2 | 1.1 | 3.0 |
| MtNis 1.21 | 0.0 | 20.3 | 63.0 | 2.5 | 1.3 | 3.0 |

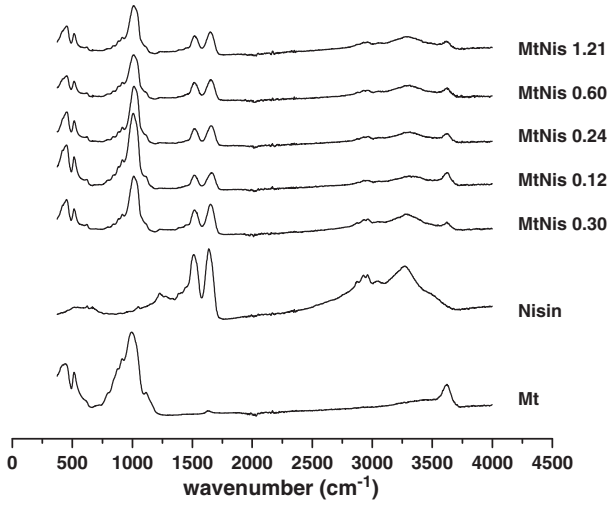


**Fig. 4.** FTIR spectra of MtNis resulting systems.

thermal changes, hydration water). OM combustion occurred between 300 and 600 °C, with two exothermic peaks at 320 °C and 360 °C, and a third broad exothermic peak near 500 °C (Fig. 6a). For the MtNis powders, both groups of DTA peaks, corresponding to pure solid and nisin, appeared in combination (Fig. 6b). With increasing NL the DTA combustion signal splits into two peaks. However, the combustion peaks of nisin (320 °C and 360 °C) are shifted to higher temperatures (360 °C and 380 °C). Moreover, the 360 °C broad peak seems to be conserved while the 380 °C peak is similar to the 320 °C peak observed for pure nisin by DTA analysis. Higher combustion peaks for organic molecules intercalated in organoclays were observed previously, indicating that more heat is required to remove the intercalated molecule (He et al., 2006a; Zhou et al., 2007). For MtNis powders, the broad peak at 360 °C could be assigned to "free" nisin combustion while the 380 °C combustion peak corresponds to the combustion of intercalated nisin, since the intensity of the signal increases with increasing NL.

The MtNis adsorption isotherm was plotted with the data obtained from TG (Fig. 6c). It can be observed that for concentrations of nisin higher than the equivalent to 0.24 CEC of Mt, a further increase of the NL value does not increase the amount of calcined OM, since saturation has already been attained. The curve reaches a plateau which is in agreement with the Langmuir theory. This equation typically describes the sorption of monolayers of high adsorbate–adsorbent interaction with

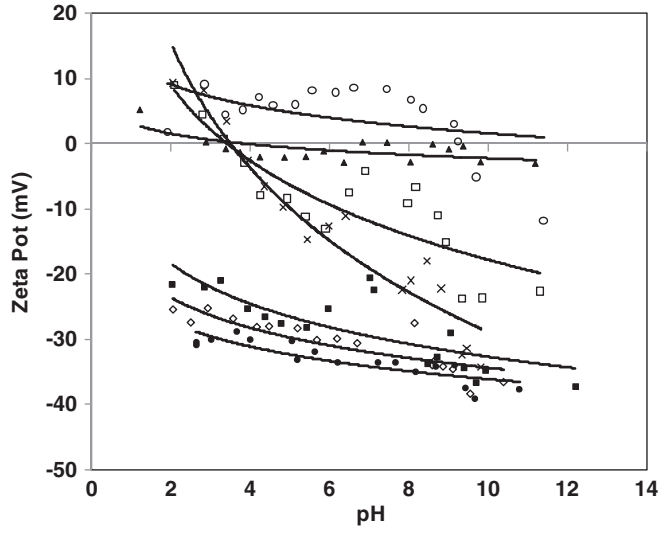


**Fig. 5.** Zeta potential titration curves of Mt (•), MtNis 0.06 (◊), MtNis 0.12 (■), MtNis 0.24 (x), MtNis 0.60 (□), MtNis 1.2 (▲) and pure Nisin (○) dispersed in KCl 0.001 M.

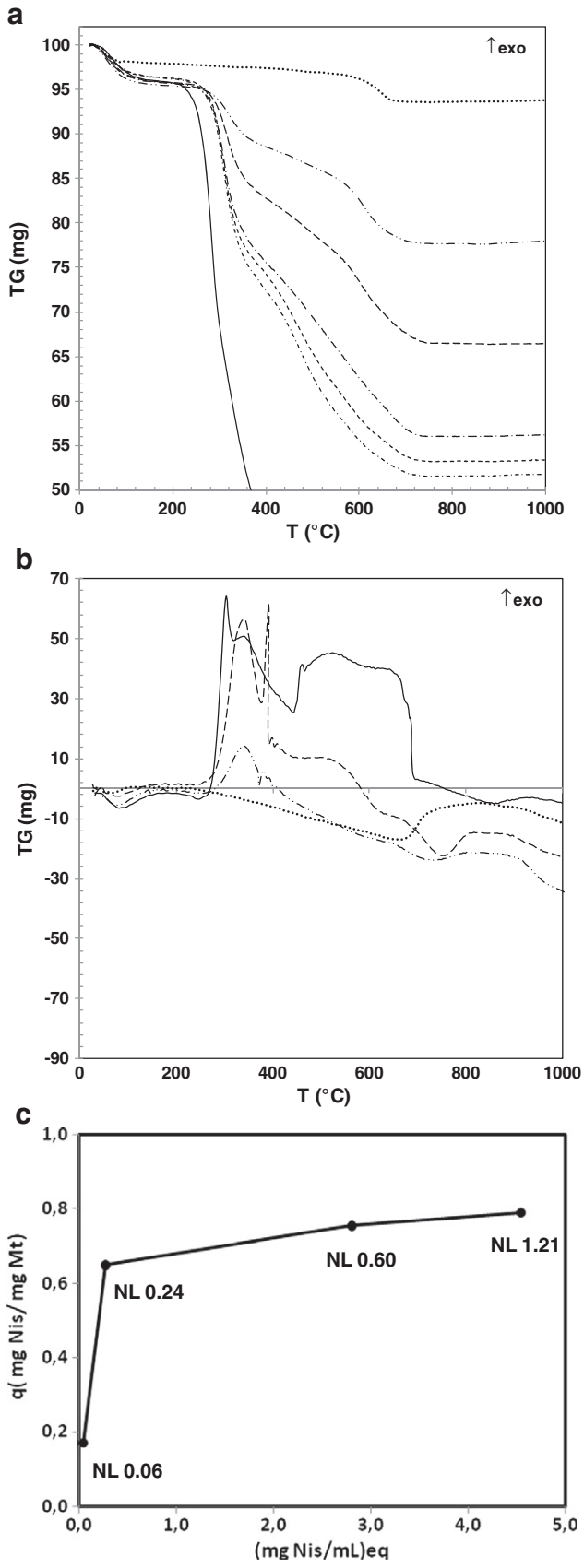


**Fig. 6.** TG (a) and DTA (b) patterns for Mt (•••), MtNis 0.06 (— — ••), MtNis 0.12 (— — —), MtNis 0.24 (— •— •), MtNis 0.60 (————), MtNis 3.0(-•-•-) and pure nisin (full line). (c) adsorption isotherm of nisin on Mt (25 °C) determined by thermogravimetric (TG) analysis.

probable specific bounding sites (Giles et al., 1974a,b). In the Langmuir linearized equation $\mathbf{C_e} / \mathbf{Q_e} = \mathbf{1} / (\mathbf{q_{max}} \cdot \mathbf{b}) + \mathbf{C_e} / \mathbf{q_{max}}$, where $\mathbf{C_e}$ (mg Nis/mL) is the final equilibrium concentration of nisin, $\mathbf{Q_e}$ (mg Nis/mg Mt) is the amount of bound nisin per unit mass of clay mineral at the final equilibrium concentration, and **b** (mL/mg Nis) is the Langmuir constant related to the affinity of binding sites, which is considered a measure of the energy of sorption; from the application of this equation an adsorption capacity ($\mathbf{q_{max}}$) of 0.80 mg Nis/mg Mt was deduced, with a Langmuir constant (**b**) of 8.20 mL/mg Nis. The Langmuir isotherm was evaluated by a dimensionless factor $R_L = 1 / (1 + b \cdot C_0)$ where $C_0$ (mg Nis/mL) is the initial nisin concentration and *b* is the Langmuir adsorption equilibrium constant. A value of $R_L = 0.02$ was obtained, indicating that the adsorption of nisin on Mt was "favorable", which was established as a valid inference for $0 < R_L < 1$ (Khotimchenko et al., 2008).

## 4. Conclusions

Montmorillonite nisin nanocomposite powders with different antimicrobial loadings were successfully obtained. The modification of Mt interlayer space, measured by XRD and TEM analyses, supports the hypothesis that nisin molecules interact with the clay mineral structure by producing a "frustrated intercalation". This intercalation model proposes a monolayer arrangement of nisin molecules between the layers located near the edges of the solid, while internal layers remain without intercalation, since they are not accessible to the large antimicrobial molecules. The adsorption isotherm obtained by TG measurements can be fitted to a Langmuir curve, strengthening the monolayer sorption scheme. FTIR assays, in combination with zeta potential and XPS measurements, also provided evidences of the intercalation of nisin molecules in the solid matrix. In addition, a NL equivalent to 0.24 CEC of Mt sets a "break line" in the behavior of MtNis systems. A plateau in the adsorption isotherm, the complete displacement of Mt intercalated sodium (EDX), and positive zeta potential values were detected for powders with NL > 0.24 CEC. Nisin concentrations exceeding 0.24 CEC of Mt are necessary to attain a complete inhibitory effect against *E. faecium* C1. DTA analysis distinguishes between the combustion of "free" and intercalated nisin in MtNis powders. The "free" nisin molecules, which are available once the saturation and displacement of sodium occur, seem to be responsible for the detected inhibition activity of MtNis powders with NL > 0.24. In conclusion, the immobilization of nisin on a raw clay mineral (Mt) represents a successful strategy to protect and ensure the gradual liberation of antimicrobial peptides; it preserves their inhibitory activity and could therefore find an application as food biopreservative.

## Acknowledgments

This work was funded by Consejo de Investigación de la Universidad Nacional de Salta (PI 1897) and the Alexander von Humboldt Foundation (Germany). C. Ibarguren thanks CONICET (Argentina) and the Alexander von Humboldt Foundation (Germany) for the fellowships. The authors are very grateful to Joss Delves-Broughton and Danisco UK Limited (England) for the kind supply of nisin; also to K. Zorn, S. Flauder, H. Garlipp, R. Wagner and D. Güttler (IMT-Friedrich-Schiller-University of Jena (Germany)) for their assistance.

## References

Acosta, E.J., Deng, Y., White, G.N., Dixon, J.B., McInnes, K.J., Senseman, S.A., Frantzen, A.S., Simanek, E.E., 2003. Dendritic surfactants show evidence for frustrated intercalation: a new organoclay morphology. Chem. Mater. 15, 2903–2909.

Audisio, M.C., Terzolo, H.R., Apella, M.C., 2005. Bacteriocin from honeybee beebread *Enterococcus avium*, active against *Listeria monocytogenes*. Appl. Environ. Microbiol. 71, 3373–3375.

Benech, R.O., Kheadr, E.E., Lacroix, C., Fliss, I., 2002. Antibacterial activities of nisin Z encapsulated in liposomes or produced *in situ* by mixed culture during cheddar cheese ripening. Appl. Environ. Microbiol. 68, 5607–5619.

Bergaya, F., Vayer, M., 1997. CEC of clays: measurement by adsorption of a copper ethylenediamine complex. Appl. Clay Sci. 12, 275–280.

Bergaya, F., Theng, B.K.G., Lagaly, G., 2006. Handbook of Clay Science, Developments in Clay Science, first ed. Elsevier, Amsterdam 717–741.

Bertagnolli, C., Kleinübing, S.J., da Silva, M.G.C., 2011. Preparation and characterization of a Brazilian bentonite clay for removal of copper in porous beds. Appl. Clay Sci. 53, 73–79.

Bower, C.K., McGuire, J., Daeschel, M.A., 1995. Suppression of *Listeria monocytogenes* colonization following adsorption of nisin onto silica surfaces. Appl. Environ. Microbiol. 61, 992–997.

Carrado, K.A., 2000. Synthetic organo- and polymer-clays: preparation, characterization, and materials applications. Appl. Clay Sci. 17 (1), 1–23.

Carretero, M.I., Gomes, C.S.F., Tateo, F., 2006. Clays and human health, In: Bergaya, F., Theng, B.K.G., Lagaly, G. (Eds.), Handbook of Clay Science, Developments in Clay Science, first ed. Elsevier, Amsterdam, pp. 717–741.

Chandrapati, S., O'Sullivan, D.J., 1998. Procedure for quantifiable assessment of nutritional parameters influencing nisin production by *Lactococcuslactis* subsp. *lactis*. J. Biotechnol. 63, 229–233.

Chen, H., Hoover, D.G., 2003. Bacteriocins and their food applications. Compr. Rev. Food Sci. Food Saf. 2, 82–100.

Čičel, B., Kranz, G., 1981. Mechanism of montmorillonite structure degradation by percussive grinding. Clay Miner. 16, 151–162.

Cutter, C.N., Siragusa, G.R., 1997. Growth of *Brochothrixthermosphacta* in ground beef following treatments with nisin in calcium alginate gels. Food Microbiol. 14, 425–430.

Daba, H., Pandian, S., Gosselin, J.F., Simard, R.E., Huang, J., Lacroix, C., 1991. Detection and activity of a bacteriocin produced by *Leuconostocmesenteroides*. Appl. Environ. Microbiol. 57, 3450–3455.

Daeschel, M.A., McGuire, J., Al-Makhlafi, H., 1992. Antimicrobial activity of nisin adsorbed to hydrophilic and hydrophobic silicon surfaces. J. Food Prot. 55, 731–735.

Dawson, P.L., Harmon, L., Sotthibandhu, A., Han, I.Y., 2005. Antimicrobial activity of nisin-adsorbed silica and corn starch powders. Food Microbiol. 22 (1), 93–99.

Deegan, L.H., Cotter, P.D., Hill, C., Ross, P., 2006. Bacteriocins: biological tools for biopreservation and shelf-life extension. Int. Dairy J. 16, 1058–1071.

Dellisanti, F., Minguzzi, V., Valdrè, G., 2006. Thermal and structural properties of Ca-rich Montmorillonite mechanically deformed by compaction and shear. Appl. Clay Sci. 31, 282–289.

Eloussaief, M., Kallel, N., Yaacoubi, A., Benzina, M., 2011. Mineralogical identification, spectroscopic characterization, and potential environmental use of natural clay materials on chromate removal from aqueous solutions. Chem. Eng. J. 168, 1024–1031.

Giles, C.H., Smith, D., Huiston, A., 1974a. A general treatment and classification of the solute adsorption isotherms. I. Theorical. J. Colloid Interface Sci. 47, 755–765.

Giles, C.H., D'Silva, A.P., Easton, I.A., 1974b. A general treatment and classification of the solute adsorption isotherms. II. Experimental interpretation. J. Colloid Interface Sci. 47, 766–778.

He, H., Yang, D., Yuan, P., Shen, W., Frost, R.L., 2006a. A novel organoclay with antibacterial activity prepared from montmorillonite and *Chlorhexidini Acetas*. J. Colloid Interface Sci. 297, 235–243.

He, H., Frost, R.L., Bostrom, T., Yuan, P., Duong, L., Yang, D., Xi, Y., Kloprogge, J.T., 2006b. Changes in the morphology of organoclays with $HDTMA^+$ surfactant loading. Appl. Clay Sci. 31, 262–271.

He, H., Zhou, Q., Frost, R.L., Wood, B.J., Duong, L.V., Kloprogge, J.T., 2007. A X-ray photoelectron spectroscopy study of HDTMAB distribution within organoclays. Spectrochim. Acta A 66, 1180–1188.

Ibarguren, C., Raya, R.R., Apella, M.C., Audisio, M.C., 2010. *Enterococcus faecium* isolated from honey synthesized bacteriocin-like substances active against different *Listeria monocytogenes* strains. J. Microbiol. 48 (1), 44–52.

Janes, M.E., Nannapaneni, R., Proctor, A., Johnson, M.G., 1998. Rice hull ash and silicic acid as adsorbents for concentration of bacteriocins. Appl. Environ. Microbiol. 64, 4403–4409.

Joshi, G.V., Patel, H.A., Kevadiya, B.D., Bajaj, H.C., 2009. Montmorillonite intercalated with vitamin B1 as drug carrier. Appl. Clay Sci. 45 (4), 248–253.

Khotimchenko, M., Kovalev, V., Khotimchenko, Y., 2008. Comparative equilibrium studies of sorption of Pb(II) ions by sodium and calcium alginate. J. Environ. Sci. 20, 827–831.

Kikouama, J.R.O., Konan, K.L., Katty, A., Bonnet, J.P., Baldé, L., Yagoubi, N., 2009. Physico-chemical characterization of edible clays and release of trace elements. Appl. Clay Sci. 43, 135–141.

Kong, J., Yu, S., 2007. Fourier transform infrared spectroscopic analysis of protein secondary structures. Acta Biochim. Biophys. Sin. 39 (8), 549–559.

Lagaly, G., Ogawa, M., Dékány, I., 2006. Clay mineral organic interactions, In: Bergaya, F., Theng, B.K.G., Lagaly, G. (Eds.), Developments in Clay Science. Handbook of Clay Science, first ed. Elsevier, Amsterdam, pp. 309–377.

Lante, A., Crapisi, A., Pasini, G., Scalabrini, P., 1994. Nisin released from immobilization matrices as antimicrobial agent. Biotechnol. Lett. 16, 293–298.

Liu, W., Jansen, J.W., 1990. Some chemical and physical properties of nisin, a small-protein antibiotic produced by *Lactococcuslactis*. Appl. Environ. Microbiol. 56, 2551–2558.

Magnoli, A.P., Tallone, L., Rosa, C.A.R., Dalcero, A.M., Chiacchiera, S.M., Torres Sanchez, R.M., 2008. Commercial bentonites as detoxifier of broiler feed contaminated with aflatoxin. Appl. Clay Sci. 40, 63–71.

Naranjo, P.M., 2012. Organoclays. Preparation, Characterization and Applications. (PhD Thesis) Faculty of Sciences. National University of Salta, Argentina.

Naranjo, P.M., Sham, E.L., Rodriguez Castellón, E., Torres Sánchez, R.M., Farfán Torres, E.M., 2013. Identification and quantification of the interaction mechanisms between the cationic surfactant HDTMA-Br and montmorillonite. Clays Clay Miner. 61, 98–106.

Park, Y., Ayoko, G.A., Frost, R.L., 2011. Application of organoclays for the adsorption of recalcitrant organic molecules from aqueous media. J. Colloid Interface Sci. 354, 292–305.

Redding, A.Z., Burns, S.E., Upson, R.T., Anderson, E.F., 2002. Organoclay sorption of benzene as a function of total organic carbon content. J. Colloid Interface Sci. 250, 261–264.
Reslow, M., Adlercrutz, P., Mattiason, B., 1988. On the importance of the support material for bioorganic synthesis. Influence of water partition between solvent, enzyme and solid support in water-poor reaction media. Eur. J. Biochem. 172, 573–578.
Servagent-Noinville, S., Revault, M., Quiquampoix, H., Baron, M.H., 2000. Conformational changes of bovine serum albumin induced by adsorption on different clay surfaces: FTIR analysis. J. Colloid Interface Sci. 221 (2), 273–283.
Thomas, L.V., Delves-Broughton, J., 2005. Nisin. In: Sofos, J.N., Branen, A.L. (Eds.), Antimicrobials in Food. CRC Press, Florida, pp. 237–274.
Wang, J.S., Luo, H., Billam, M., Wang, Z., Guan, H., Tang, L., Goldston, T., Afriyie-Gyawu, E., Lovett, C., Griswold, J., Brattin, B., Taylor, R.J., Huebner, H.J., Phillips, T.D., 2005. Short-term safety evaluation of processed calcium montmorillonite clay (NovaSil) in humans. Food Addit. Contam. 22 (3), 270–279.
Were, L.M., Bruce, B., Davidson, P.M., Weiss, J., 2004. Encapsulation of nisin and lysozyme in liposomes enhances efficacy against *Listeria monocytogenes*. J. Food Prot. 67, 922–927.
Yang, D., Yuan, P., Zhu, J.X., He, H.P., 2007. Synthesis and characterization of antibacterial compounds using montmorillonite and chlorhexidine acetate. J. Therm. Anal. Calorim. 89 (3), 847–852.
Zhou, Q., Frost, R.L., He, H., Xi, Y., Zbik, M., 2007. TEM, XRD, and thermal stability of adsorbed paranitrophenol on DDOAB organoclay. J. Colloid Interface Sci. 311, 24–37.
Zhou, Q., He, H., Frost, R.L., Xi, Y., 2008. Changes in the surfaces on DDOAB organoclays adsorbed with paranitrophenol—an XRD, TEM and TG study. Mater. Res. Bull. 43, 3318–3326.
Zhu, J.X., He, H.P., Guo, J.G., Yang, D., Xie, X.D., 2003. Arrangement models of alkylammoniumcations in the interlayer of $HDTMA^+$ pillared montmorillonites. Chin. Sci. Bull. 48, 368–372.